African Journal of Biological Sciences

Journal homepage: http://www.afjbs.com

Research Paper   Open Access

"Synergistic Treatment of Effluent: Investigating the Interaction between Powdered Wool and Malachite Green"

Kiran M. Lalge[1,4], Malhari C. Nagtilak[2], Vidyarani S. Patil[1,5],
Sandip N. Labade[1,2], Nilesh J. Khengare[1], Shkuntala S. Sawant[1,3],
Ranjana K. Jadhav[1*]

[1]Research Centre in Chemistry, S. M. Joshi College, Pune - 411028, Maharashtra, India.
[2]Dr. B. N. Purandare Arts, Smt. S. G. Gupta Commerce and Science College, Lonavala-410403, Maharashtra, India.
[3]R. S. B. Mahavidyalaya Aundh-Khatav - 415510, Maharashtra, India.
[4]Jayawantrao Sawant Commerce and Science College, Pune-411028, Maharashtra, India.
[5]Yashwantrao Chavan Institute of Science, Satara 415001, Maharashtra, India
*Correspondence author: Ranjana. K. Jadhav email: rkjadhav@smjoshicollege.edu.in

Abstract

Natural wool undergoes carbonization, resulting in a powdered form utilized as an adsorbent in its interaction with Malachite Green (MG) for wastewater treatment purposes. The pH, temperature, concentration of MG, quantity of powdered wool, particle size of powdered wool, and required contact time were studied with respect to batch. The dye was largely removed by treating the area with an adsorbent and then filtering the mixture through a syringe filter. The highest level of interaction was observed within the pH range of 9 to 10. The interaction of powdered wool and MG has been observed to be endothermic in nature. Chemisorption type interaction characterizes the process. The experimental data align most accurately with the Langmuir adsorption model. Thermodynamic variables including ΔH, ΔG, and ΔS were also computed for the interaction between MG and powdered wool. The process was observed to follow pseudo-second-order kinetics. Efforts have also been undertaken to reclaim the MG utilizing a solution of weak hydrochloric acid, yielding a dye recovery rate of 95%.

Keywords: Powdered wool, Malachite Green, Adsorption isotherms, Kinetics, Thermodynamics, Molecular docking.

1. Introduction:

The interaction between polymers and dyes is a key point in various fields such as papers, textiles, coatings, and environmental remediation. Polymers can adsorb dyes onto their surface through various mechanisms, including physical adsorption, chemical binding, or a combination of both [1]. Physical adsorption encompasses non-covalent connections like van der Waals forces and hydrophobic interactions, whereas chemical adsorption entails covalent bonding, hydrogen bonding, and ionic bond formation between the polymer and dye molecules [2].

MG dye has historically been used to dye textiles, including cotton, silk, and wool [3]. This method finds frequent application in the Gram staining procedure to distinguish between Gram-negative and Gram-positive bacteria [4]. MG has been employed in aquaculture to manage parasitic and fungal infections in fish eggs and fish [5]. This dye has been used in veterinary medicine to treat fungal infections in animals, including farm animals and pets [6]. MG has applications in biological research, including its use as a stain for visualizing nucleic acids such as DNA and RNA in gel electrophoresis techniques [7].

MG has been reported as a potential human carcinogen [8]. It has been shown to exhibit mutagenic properties [9] and is highly toxic to aquatic organisms, including fish and invertebrates [10]. MG has been communicated to respiratory toxicity [11].
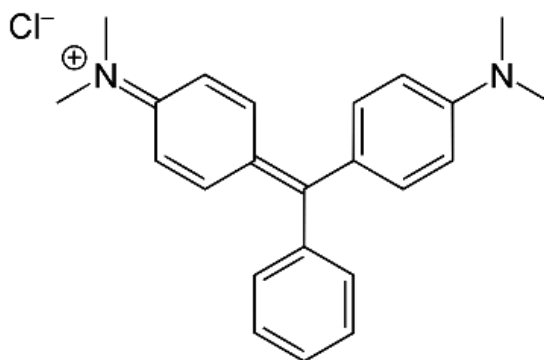

Fig. 1. Structure of Malachite Green.

Collectively, the removal of MG from effluent is essential to protect the environment, human beings, and maintain water quality standards. Effective wastewater treatment processes can help mitigate the impact of MG contamination and ensure the sustainability of water resources.

Observations have noted the use of various materials, such as activated carbon from rice husks [12], bottom ash [13], hen feathers [14], activated carbon derived from Borassus aethiopum flowers [15], oil palm trunk fiber [16], treated sawdust [17], activated carbon prepared from bamboo [18], rice straw-derived char [19], rattan sawdust [20], bentonite clay [21], cyclodextrin [22], aggressive seaweed species Caulerpa racemosa var cylindracea [23], dead leaves of plane trees [24], tin oxide nanoparticle-loaded materials [25], and halloysite nanotubes [26], etc., for the elimination of MG from effluent.

This work suggests the use of powdered wool for the interaction with MG to treat effluent, aiming to introduce powdered wool, a simple and readily available material, for the elimination of MG from effluent.

2. Experimental:

2.1. Material development:

Wool was collected from a single sheep owned by a local shepherd. In the first stage, the wool was carbonized using sodium carbonate and hydrochloric acid. Distilled water was used for cleaning. Subsequently, the wool was cut into tiny particles and powdered. The resulting wool powder was utilized as an adsorbent in further studies. Various mesh sizes, specifically 125, 150, and 180 BSS mesh, were employed to sieve the wool. The resulting powdered wool was stored in a desiccator.

2.2. Preparation of dye solution:

Malachite Green Oxalate ("ammonium, (4-(p-(dimethylamino)-alpha-phenylbenzylidene)-","2,5 cyclohexadienylidene) dimethyl, oxalate (2:1), oxalate (1:1) ", "C.I.42000" (Molecular formula $C_{52}H_{54}N_4O_{12}$ and molecular weight 927.01 g/mol) was purchased from Otto chemicals. A stock solution was prepared using MG dye, resulting in a concentration of 5000 mg/L. The necessary working solutions were subsequently formulated through the dilution of the original solution using distilled water.

2.3. Instrumentation:

A model LI 120 (Elico Instruments, India) of pH meter with a microprocessor was used to measure the pH. Using a UV-visible spectrophotometer (Shimadzu UV-1800), the absorption spectrum was measured. The analysis of powdered wool and wool-malachite green composite using FESEM was conducted on the FEI Nova NanoSEM 450. The FTIR spectra (JASCO FTIR-4600) employing the KBr pellet technique were utilized to measure the characteristics of wool-Malachite Green composite, wool, and MG. The analysis of the TGA of the wool-malachite green composite was conducted using TGA Instruments Trios V4.4.0.41128. The investigation of powdered wool using the Brunauer-Emmett-Teller (BET) method was performed with the Quantachrome Instruments Autosorb iQ Station 2 version 3.01.

2.4. Interaction studies:

At a temperature of 30°C and specific pH levels, batch studies were conducted by placing 10 mL of a dye solution with a known concentration into a 50 mL volumetric flask. The studies involved varying the concentration of MG, the pH of the solution, the contact time, the amount of powdered wool, etc., after determining the appropriate mesh sizes for the adsorbent materials. After a specific duration, the solutions were filtered using cellulose nitrate membrane filter paper (pore size 0.22 μm) and subsequently analyzed spectrophotometrically at a wavelength of λmax 622 nm.

2.5. *Optimization of variables:*

The interaction of MG and powdered wool was studied by investigating the effects of solution pH, contact time, particle size, temperature, amount of powdered wool, MG concentration, dye desorption, and molecular docking.

2.5.1. *Interaction with respect to the effect of pH:*

A 50 ml conical flask was filled with a 10 ml solution of MG at a concentration of 100 mg/L, adjusted to a pH range of 1.0-10.0. At 30°C, 100 mg of powdered wool with a mesh size of 90-120 was added to the mixture and swirled for two minutes. The solution was filtered using a syringe filter equipped with porafil paper. Following the protocol, spectrophotometric analysis of the filtrate was performed. The plot of percent adsorption of MG versus pH is shown in **Fig. 1.**
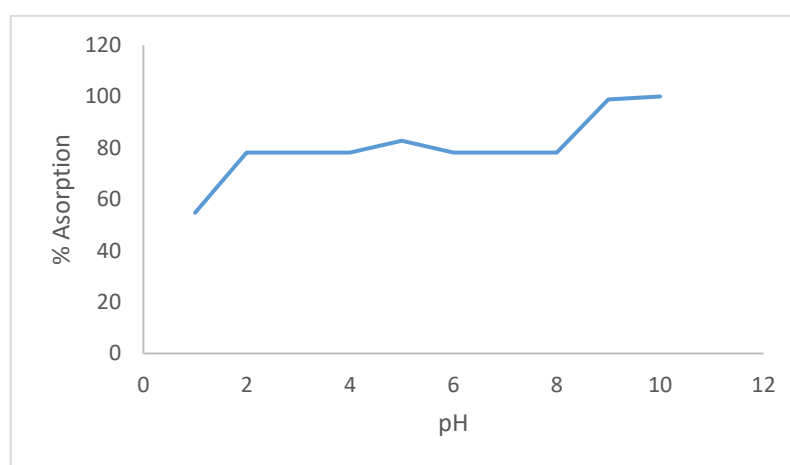

Fig. 1. Impact of pH of dye solution on adsorption at 30ºC and 100 mg/l dye concentration. Adsorbent dose 100 mg/10 ml; Particle size 125-150 mesh.

2.5.2. *Effect of contact time:*

A 10 ml solution containing 100 mg L^{-1} of MG was placed into a 50 ml conical flask at pH 10. Wool powder (100 mg, 90–150 µm) was added to the solution and stirred for five to thirty seconds at 30°C. The mixture was then filtered using a syringe filter with porafil paper. The collected filtrate was subsequently analyzed spectrophotometrically. The plot of the percentage adsorption of MG versus time is presented in **Fig. 2.**
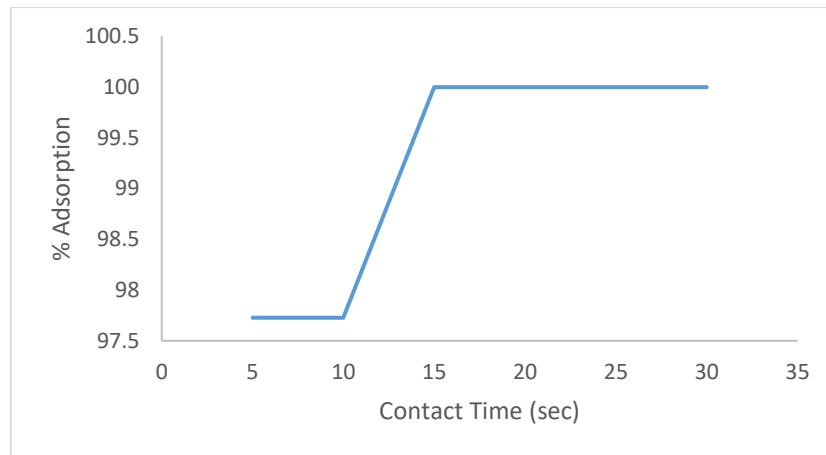
Fig. 2: Impact of contact time on dye adsorption

2.5.3. *Effect of Variation of particle size on interaction powdered wool and MG:*

A 50 mL conical flask was filled with a 10 mL solution containing 100 mg/L of MG at pH 10. The solution of MG and powdered wool was agitated with particle sizes <90 µm, 90–150 µm, 150–180 µm, and >180 µm for 15 seconds at 30°C. The wool adsorbed with MG was collected, and the MG concentration of the collected filtrate was determined spectrophotometrically. The plot of the percentage adsorption of MG versus time is shown in **Fig. 3.**
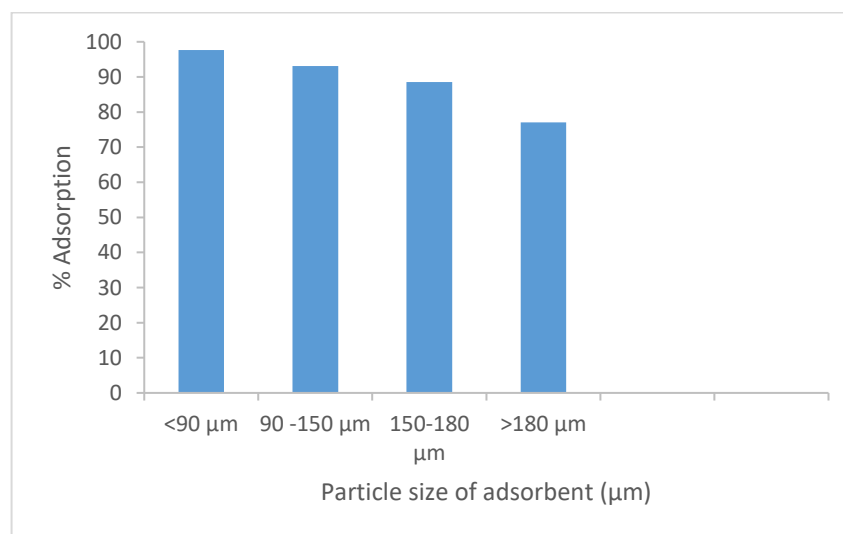

Fig. 3. Consequences of particle size of adsorbent on adsorption at 30$^\text{O}$C, 100 mg/l dye concentration, and pH=10, adsorbent dose 100 mg/10 ml

2.5.4. *Temperature shows impact on powdered wool MG interaction:*

The aliquot (10 ml) of the solution (100 mg/L of MG) at pH 10 was shaken for 15 s at different temperatures ranging from 10°C to 60°C with 100 mg of powdered wool (90–150 µm). As specified in the protocol, spectrophotometry was used to analyze the filtrate. **Fig. 4** shows the curve of the percentage of MG adsorption against temperature.
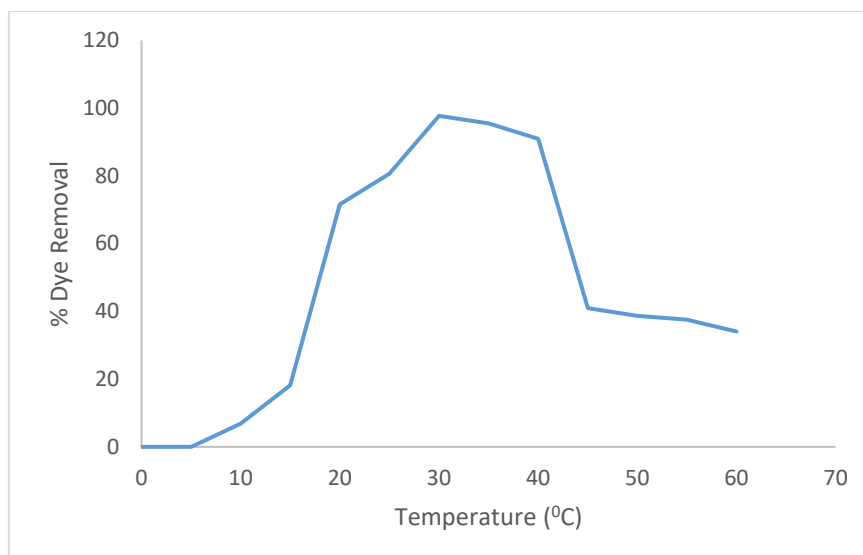
Fig. 4: **Graph of Temperature vs Dye Removal**

2.5.5. *Effect of amount of adsorbent:*

A 50 ml conical flask containing the solution (10 ml, 100 mg/L of MG) at pH 10 was used. Powdered wool with sizes ranging from 90 to 150 µm was shaken for 15 seconds at 30°C. The wool that had adsorbed MG was collected, and spectrophotometry was used to measure the amount of MG in the filtrate. **Fig. 5** shows the curve of the percentage of MG adsorption versus the quantity of powdered wool.
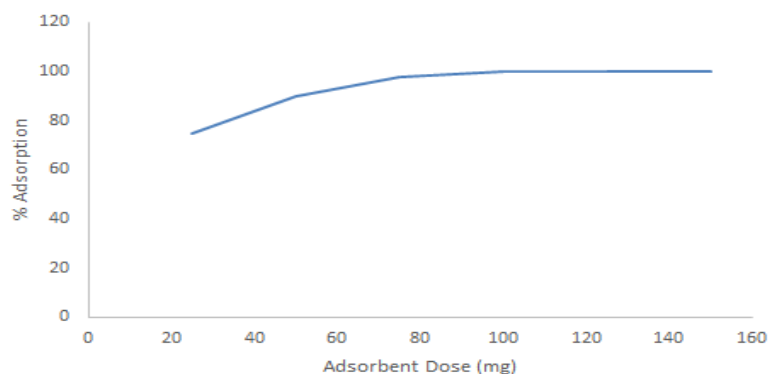

Fig. 5. Effect of amount of adsorbent on adsorption at 30$^{\text{o}}$C, 100 mg/l dye concentration, and pH=10

2.5.6. *MG concentration effect on interaction:*

A 50 ml conical flask was filled with a 10 ml solution containing MG at concentrations ranging from 50 to 200 mg/L at pH 10. The flask was then stirred for 15 seconds at 30°C using 100 mg of powdered wool (90–150 µm). The wool-MG composite in powder form was collected. Using spectrophotometry, the MG concentration in the filtrate was examined. **Fig. 6** shows the curve of the percentage

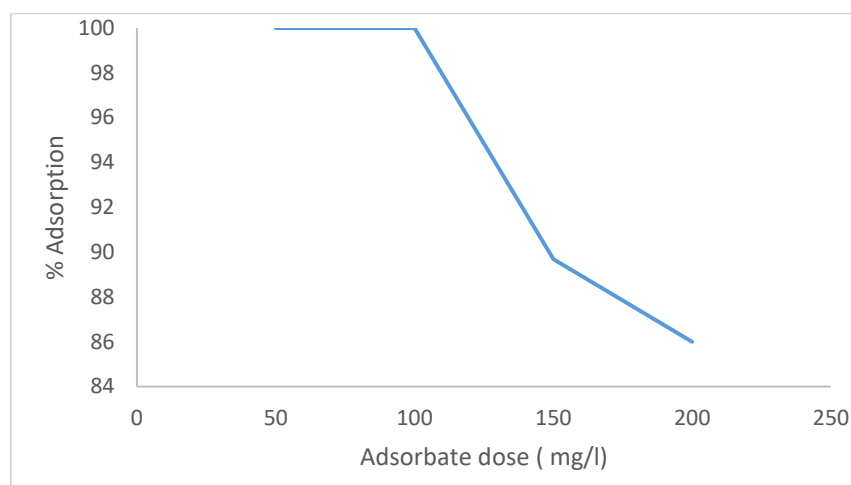of MG adsorption against its concentration.

Fig. 6. Effect of concentration of dye on adsorption at 30$^{\text{o}}$C, and pH = 10, Adsorbent dose 100 mg/10 ml

2.5.7. *Dye Recovery studies:*

Using a magnetic stirrer, solutions ranging from pH 1.0 to 10.0 were added to the powdered wool containing adsorbed MG and stirred for 5 minutes at 30°C. Following the MG's desorption, the powdered wool was fractioned by filtering, and the amount of MG was determined using a spectrophotometer. **Fig. 7** displays the percent desorbed **vs.** pH graph.
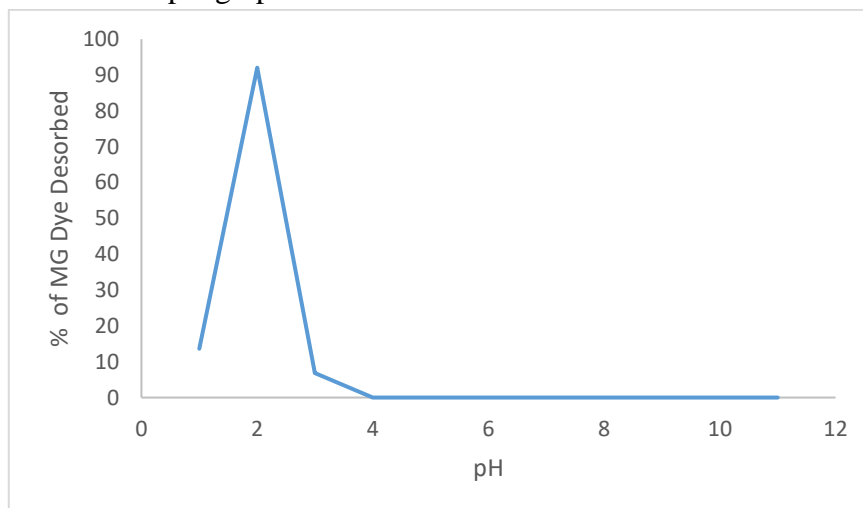

Fig. 7. **Effect of pH on desorption of MG from powdered wool.**

2.5.8. *Molecular docking studies:*

The Protein Data Bank provided the molecular structure of keratin in pdb format (PDB ID: 4ZRY) [27]. The obtained structure of Keratin was subjected to protein preparation using Schrodinger's Protein Preparation Wizards. The structure of MG (PubChem CID: 11295) was downloaded from the PubChem database. The preparation of ligand was done. Discovery Studio with CHARMm force field is

applied for energy minimization to get lowest energy conformation. LibDock module from Discovery Studio was employed for docking studies [28]. The binding site for Keratin was defined using Discovery Studio software by considering the whole protein, i.e., in this work we have performed blind docking calculations. For the purpose of calculating 10 runs of the Lamarckian Genetic Algorithm (LGA), the docking parameters have been improved. Two and seven thousand generations were the targets for energy evaluations. 150 was established as the population size, and 0.02 and 0.8 were chosen as the gene mutation and crossover rates, respectively [29]. The final Keratin-MG conformations were compiled and extracted utilizing as per the LibDock score and interaction patterns. To visualize the findings, the Maestro program (Schrodinger 2020-2) was used.

3. Results and discussion:
3.1. Optimization of parameters:
3.1.1. Effect of pH:

MG is a basic dye, which is inherently cationic and positively charged. The effects of pH on MG adsorption onto powdered wool were investigated within the pH range of 1.0–10.0. At pH 1, adsorption is minimal. Between pH 2 and 8, adsorption remains constant. However, at pH 9 and 10, adsorption reaches its maximum (Fig. 1). At high pH levels, the number of negatively charged adsorbent sites increases, while the number of the positively charged surface sites decreases. This promotes electrostatic attraction, facilitating the preferential adsorption of positively charged dye cations onto the surface [30]. Another potential mode of adsorption could be ion exchange [31]. Additionally, at low pH, excess H+ ions compete with dye cations, leading to reduced adsorption [32].

3.1.2. Effect of contact time:

Increased contact time correlates with heightened adsorption levels for powdered wool. After 20 seconds, adsorption remained constant. Within the initial 20 seconds of interaction, the dye achieved an adsorption rate approaching 98-100% **(Fig. 2).** The pseudo second-order chemisorption's kinetic rate equation is expressed as

$$t/q_t = 1/(k_2 q_e^2) + t/q_e \qquad ....(1)$$

Where, qt is the quantity of MG adsorbed on powdered wool at time t, q_e is the equilibrium amount of MG adsorbed, k_2 is rate constant, and t is time in minutes.

To elucidate the kinetic mechanism governing the adsorption process, the pseudo-second-order model was employed for testing. An R^2 value of 0.9999 was obtained, indicating the validity of equation (1). The kinetics of MG adsorption onto powdered wool are illustrated in **Fig. 8**.
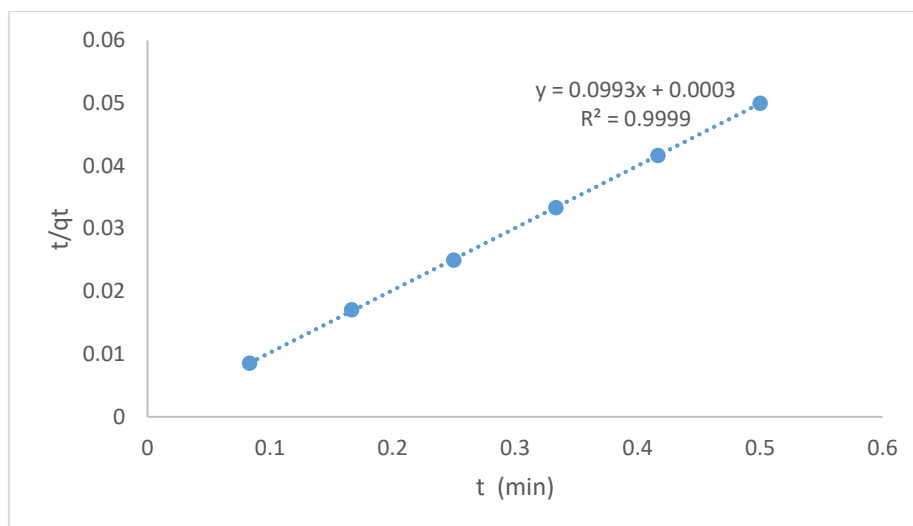
Fig. 8: Interaction of Malachite Green on Powdered Wool: Linear Pseudo Second Order Model

3.1.3. Effect of powdered wool particle size:

To study the effect of particle size, three different particle sizes, namely <90 µm, 90-150 µm, 150-180 µm, and >180 µm, were selected. With the increase in particle size, a variation in the quantity of adsorbed dye became evident (Fig. 3), presenting the impact of particle size of powdered wool on the interaction at 30°C. It was observed that adsorption enhances with a decrease in particle size. This is attributed to the enlargement of the adsorbent's surface area and the availability of active functional groups in the dye.

3.1.4. Effect of temperature on MG adsorption:

The affinity between powdered wool and MG dye has intensified with increasing temperatures ranging from 10°C to 40°C. The maximum dye adsorption is observed at 30°C **(Fig. 4)**. Beyond 30°C, adsorption decreases as the interaction between MG and powdered wool diminishes. The adsorption theory revealed that there is a decline in adsorption with an increase in temperature, and at high temperatures, desorption of adsorbed molecules occurs.

3.1.5. Effect of amount adsorbent:

To elucidate the influence of powdered silk, a range of quantities (0.05 g – 0.150 g) of powdered wool were selected for analysis. The study was conducted at 30°C, with a concentration of 100 mg/l of MG and a pH of 10. It has been discovered that the quantity of powdered wool positively enhances the interaction between MG and powdered wool **(Fig. 5)**.

3.1.6. Effect of adsorption isotherm, MG concentration, and thermodynamic properties:

The influence of MG concentration was studied with **a** constant magnitude of adsorbent dose at 30°C. Experiments reflect that at low concentrations of MG, the

extent of adsorption increases in the case of powdered wool **(Fig. 6).** The quantity of adsorbed MG at equilibrium, q_e (mg/g) was computed by

$$q_e = \frac{(Co-Ce)v}{w} \quad \text{…………...} \quad (2)$$

The quantity of adsorbed MG at time t, q_t (mg/g) was computed by

$$q_t = \frac{(Co-Ct)v}{w} \quad \text{……….} \quad (3)$$

where Co and Ce (mg/l), respectively, stand for the initial and equilibrium concentrations of MG dye in the liquid phase. V is the volume of solution (L), and w is the quantity of dry powdered wool used (g).

3.1.6.1. Adsorption isotherm:

Freundlich**,** and Langmuir isotherm models were employed for the studies. The Langmuir isotherm model equation is

$$\frac{Ce}{qe} = \frac{1}{KL.qm} + \left(\frac{1}{qm}\right) Ce \qquad \text{(Linear form)} \qquad \text{……}(4)$$

As,

C_e = Equilibrium concentration of Malachite Green oxalate dye (mgl^{-1})

q_e = Amount of oxalate dye, Malachite Green, adsorbed at equilibrium (measured in mg g^{-1})

q_m = Optimal adsorption capacity of Malachite Green Oxalate dye (mg g^{-1})**,** and

K_L = Langmuir adsorption constant (L.mg^{-1})

Fig. 9 displays the plot of Ce/qe versus Ce for the interaction of Malachite Green Oxalate dye and powdered wool. The acquired values are summarized in Table 1. **Fig. 9** illustrates the linear nature of the Langmuir isotherm model. A q_m value of 17.98 mg g^{-1} was determined. Conformance with the Langmuir model is indicated by the coefficient (R^2), which was observed to be 0.9792. The results show monolayer coverage on the adsorbent surface, indicating that the Langmuir isotherm and the adsorption data fit well with each other.

By taking into consideration the logarithmic variation of surface energy with surface coverage, the Freundlich adsorption isotherm specifies data on multilayer adsorption on a variety of surfaces. Often expressed as follows, this isotherm **is**:

$$\ln q_e = \ln K_F + \frac{1}{n \ln Ce} \qquad \text{(linear form)} \qquad \text{….. (5)}$$

Here,

K_F = Capability of the adsorption (L mg^{-1}) and

n = Magnitude of the adsorption (mg L^{-1}).

The graph $\ln q_e$ vs. $\ln C_e$ gave a linear relationship **(Fig. 10)**. In Table 1, the constants evaluated from the graph are tabulated.

Table 1: Different constants of adsorption models for the adsorption of MG dye on powdered wool:

Isotherm models	Constants of adsorption models		R^2
Langmuir	K_L =1.549 L mg^{-1}	q_m = 17.98 mg g^{-1}	0.9792

Freundlich	$K_F = 9.765$ L mg^{-1}	$n = 5.646$ mg L^{-1}	0.9537

y = 0.0556x + 0.0359
R² = 0.9792
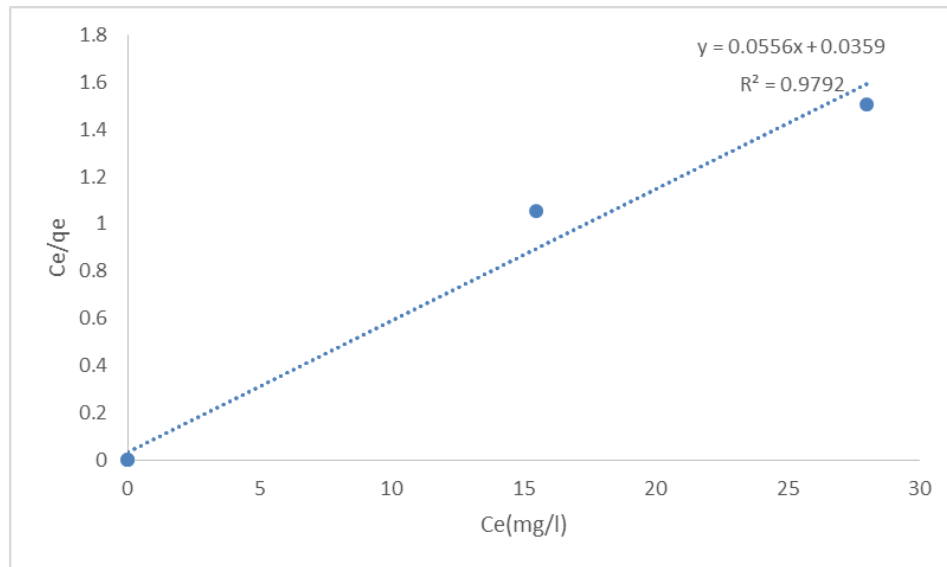
Fig. 9: Plot of Langmuir isotherm model for the wool-Malachite Green Oxalate interaction

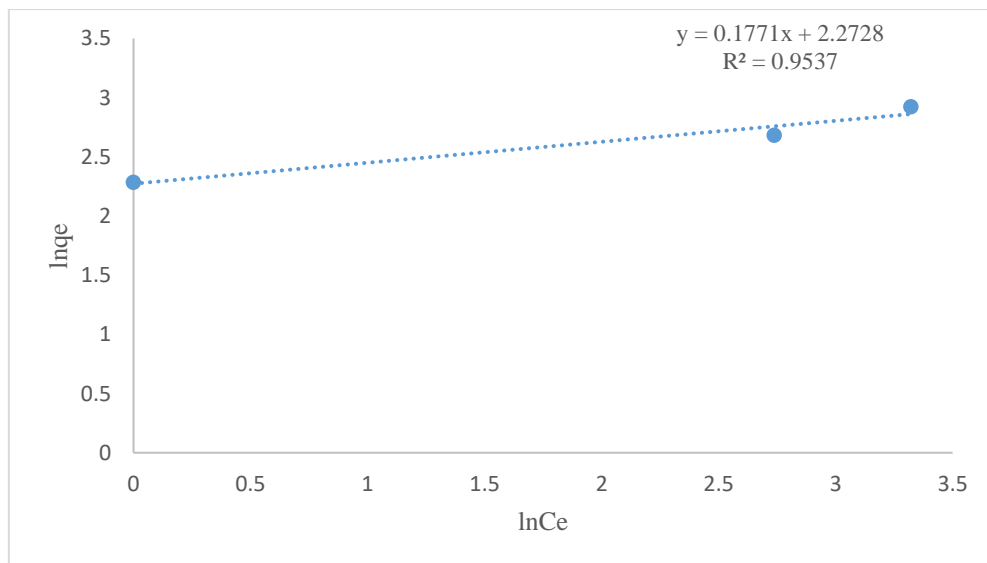y = 0.1771x + 2.2728
R² = 0.9537

Fig. 10: Plot of Freundlich isotherm model for the wool-Malachite Green Oxalate interaction

3.1.6.1. Thermodynamic properties:

As the temperature increased from 30°C to 60°C at pH 10, the adsorption of MG on powdered wool diminished, as depicted in Fig. 4. The results indicate that physisorption decreases with a rise in temperature. This phenomenon occurs because the increase in temperature weakens and subsequently detaches previously adsorbed particles due to the breaking of weak Van der Waals bonds between them. This

observation suggests the involvement of an exothermic mechanism. Typically, adsorption processes exhibit an exothermic nature, but in this case, it is endothermic due to a greater detachment of water molecules compared to the adsorption of dye molecules. Consequently, the entire interaction becomes endothermic [33].

Using Eq. (6), the change in Gibbs free energy at equilibrium was calculated. This, as was covered in the section above on the Langmuir isotherm, entails calculating the equilibrium constant (K_L).

$$\Delta G = -RT \ln K_L \qquad \text{........ (6)}$$

The absolute magnitude of ΔG may provide information regarding the type of adsorption. Physical sorption has an energy range of 0 to (-20) kJ per mole, whereas chemisorption has an energy range of -80 to -400 kJ. The ΔG value of -5.926 kJ/mol demonstrates physisorption for the adsorption of MG onto powdered wool and indicates a spontaneous nature for the adsorption. The positive value of ΔS indicates an increase in the disorder of the system. Fundamentally, the adsorption of MG molecules onto powdered wool decreases the level of entropy. However, since the process involves the desorption of water molecules, which are more abundant than dye molecules, solvent desorption contributes more to the total entropy change than dye molecule adsorption does. Furthermore, one may use the value of ΔH to distinguish between the chemisorption process (20.9-418.4 kJ/mol) and the physisorption process (2.1–20.9 kJ/mol). Within this investigation, the ΔH value of adsorption of MG Oxalate on powdered wool suggests a chemisorption process. The plot of ln K_L **vs.** 1/T, **is** shown in **Fig. 11**, is straight with a negative slope, providing a clear idea about the thermodynamic properties.

Table 2: Thermodynamics parameters for the adsorption of MG dye on powdered wool:

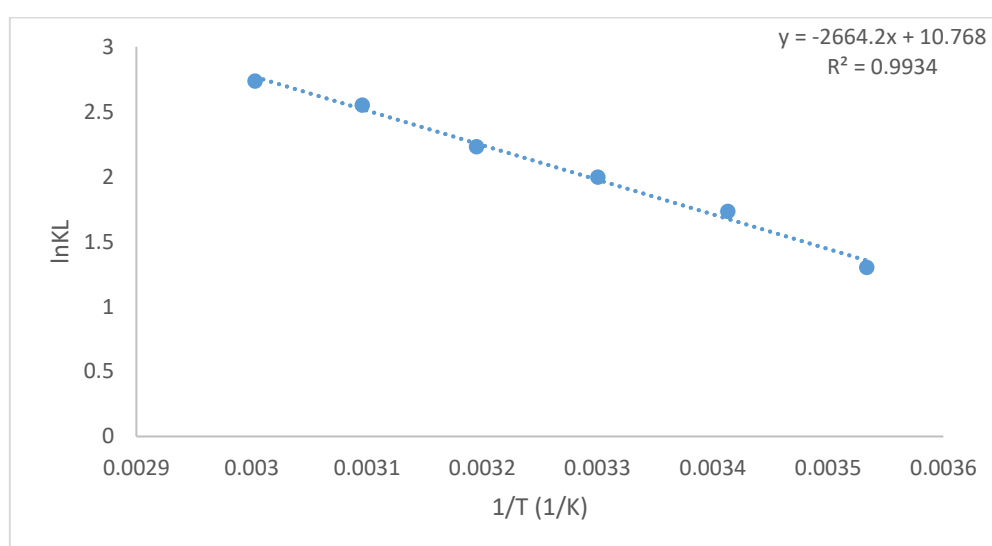| Adsorbent	ΔH (kJ/ mol)	ΔS (J/mol K)	ΔG (kJ/mol)	R^2
Powdered wool	22.158	89.525	-5.926	0.9934

Fig. 11: van't Hoff plot for the thermodynamic parameters of interaction of Malachite Green Oxalate on powdered wool

3.1.7. *Dye Recovery studies:*

Due to its ability to replenish its adsorbing capability under favorable circumstances, powdered wool is considered a promising adsorbing material. The impact of pH on MG desorption from powdered wool is depicted in **Fig. 7.** At pH 2 (HCl), desorption of MG from powdered wool was plotted in **Fig. 7.** The acidic condition alters the surface charges, causing detachment of MG from powdered wool. At pH 2, 95% removal of dye was observed, resulting in a percentage recovery of MG of 95%.

3.1.8. *Molecular docking simulation of MG-Powdered wool interaction:*

In this study, we examined the interaction between MG (ligands) and powdered wool (receptor) using computer-aided molecular docking. Each of the ligands (MG) had a charge of +1 when they were analyzed in their cationic state. The structure of powdered wool was constructed and optimized at the molecular mechanical level using the CHARMm force field. Keratin, a skeletal protein with pdb id (4ZRY), was utilized in the docking studies [35]. The binding sites of MG (CID 11295) to powdered wool were computed by molecular docking simulations. One hundred poses were used for the docking experiments, after which clustering analysis was applied [36]. The molecular docking results for geometry-optimized MG and keratin were evaluated using the scoring function. The amino acids LEU B: 437, ALA B: 440, LYS B: 441, LEU B: 444, GLN A: 403, LEU A: 404, GLN A: 406, ILE A: 407, and GLN A: 410 were found to be surrounded by MG. Among these amino acids, LYS B: 441 showed a π-cation interaction with MG. Some prominent results were interpreted in **Fig. 12.**
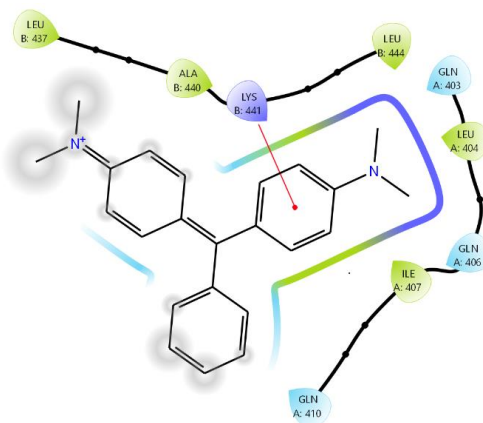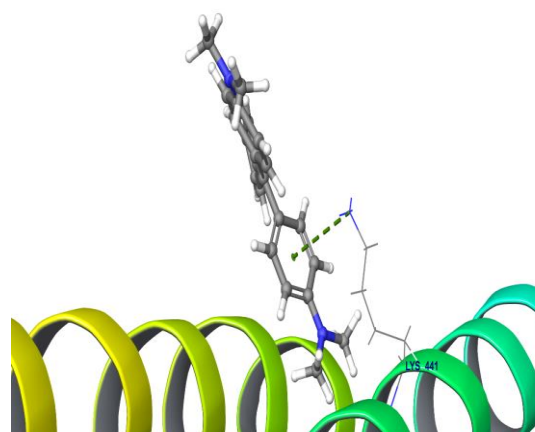

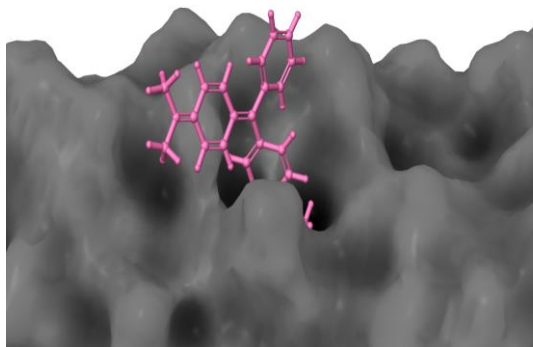**Fig. 12a 2D Keratin-MG Image**   **Fig. 12b 3D Keratin-MG Image**
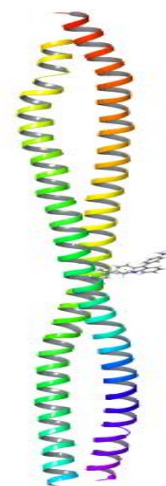
Fig. 12c Keratin-MG Cavity Image   **Fig. 12d Full Keratin-MG Image**

Fig. 12: Molecular docking interactions between Powdered wool (Keratin) and MG

3.2. Instrumental Analysis:

Conventional spectroscopic methods and available analytical techniques are employed for the analysis of powdered wool both pre- and post-adsorption **(Fig. 13).**

3.2.1. Interpretation of interaction using FT-IR:

FT-IR was employed to evaluate the chemical moieties of powdered wool, Malachite Green, and wool-Malachite Green Oxalate. The FT-IR data of the fine wool powder **is** depicted in **Fig. 13**.
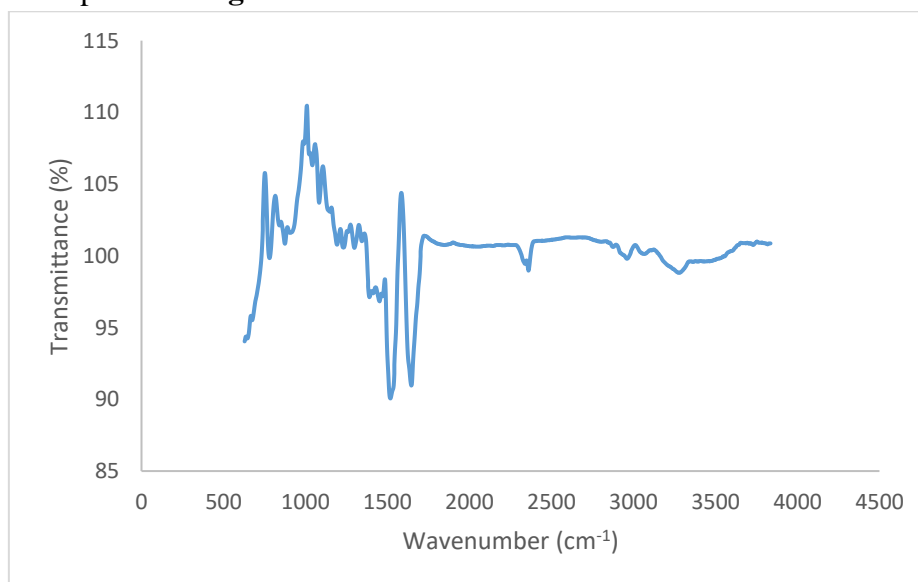

Fig. 13. FT-IR spectra of fine wool powder

The FTIR spectra of wool were noted. The moderate absorption at 782.92, 875.52 cm^{-1} showed –CH$_2$ of wool. The medium absorption at 1135.86, 1230.36,

1297.86 cm^{-1} showed amide III band, -NH bending of wool. The medium absorption at 1448.27cm^{-1} showed –CH, -CH$_2$ aliphatic bending of wool. The strong and intense absorption at 1515.77 showed amide –II linkage and 1643.05 cm^{-1} showed amide I of β-plated sheet of wool. The medium absorption at 2958.26 cm^{-1} showed amide –NH stretching of wool. The absorption at 2360 cm^{-1} showed N-H stretching, -C=N stretching of wool. The medium absorption of amide (-NH) was obtained at 3284.17 cm^{-1}. The FT-IR spectra of Malachite Green Oxalate was explained in **Fig. 14**.
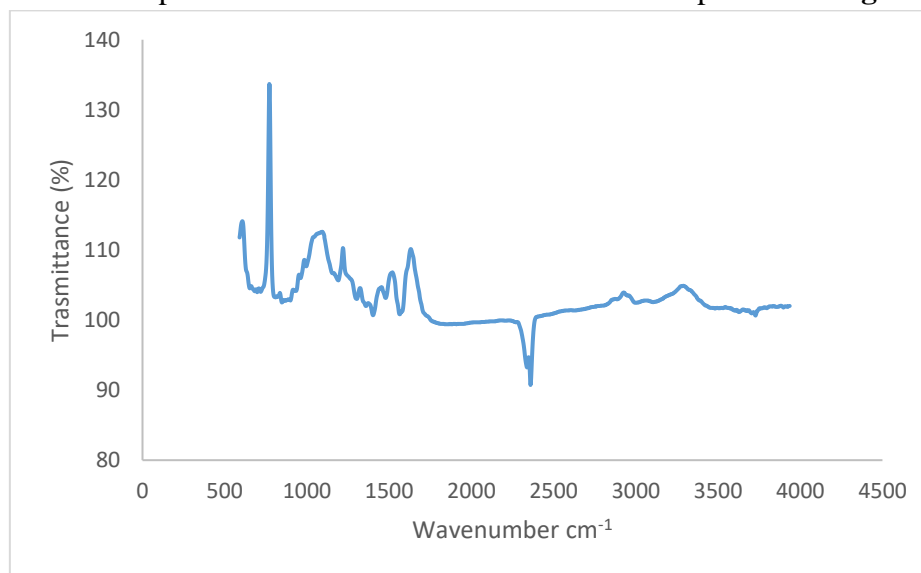

Fig. 14. FT-IR spectra of Malachite green

The FTIR absorption of Malachite Green Oxalate was noted. The medium absorption at 1189.89, 875.52 cm^{-1} illustrated C-N stretching frequency of tertiary amine. The strong absorption at 1347.99 cm^{-1} indicated C-N stretching frequency of aromatic tertiary amine. The medium absorption at 1563.97 cm^{-1} exhibited C=C stretching frequency of aromatic ring. The medium absorption at 3004.55 cm^{-1} showed C-H stretching frequency of –CH$_3$ of MG Oxalate. The FT-IR spectra of the wool-Malachite Green Oxalate interaction was presented in **Fig. 15**.
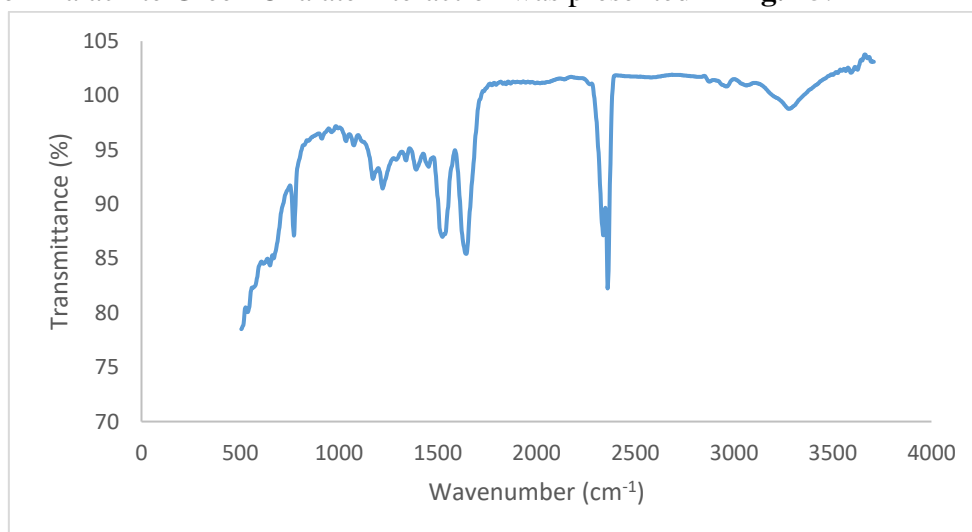

Fig. 15. FT-IR spectra of wool-Malachite Green interaction

The FTIR of powdered wool-Malachite green oxalate was captured. The medium absorption at 1078.01 and 1220.71 cm^{-1} revealed C-O stretching frequencies. The intense absorption at 1388.47 cm^{-1} displayed C-N stretching frequency of aromatic tertiary amine. The medium absorption at 1523.48 and 1646.91 cm^{-1} showed C=C stretching frequency of aromatic ring. The broad, strong absorption at 3291.89 cm^{-1} showed intermolecular hydrogen bonding in wool-Malachite Green Oxalate composite.

3.2.2. SEM data of Wool and wool-Malachite Green Oxalate composite:

SEM represents the morphology of all adsorbents. **Fig.16** represents the morphology of wool. The SEM images gave an idea about particle size of fine wool as presented in **Fig. 16**. The SEM demonstrated that the particle size of fine wool, as interpreted in **Fig. 16 and 17**, were less than 200 µm, 100 µm, and 20 µm. The powdered wool's SEM pictures showed a porous network, a grouped and uneven surface structure, and minute particles that looked like fibers (**Fig. 16).**
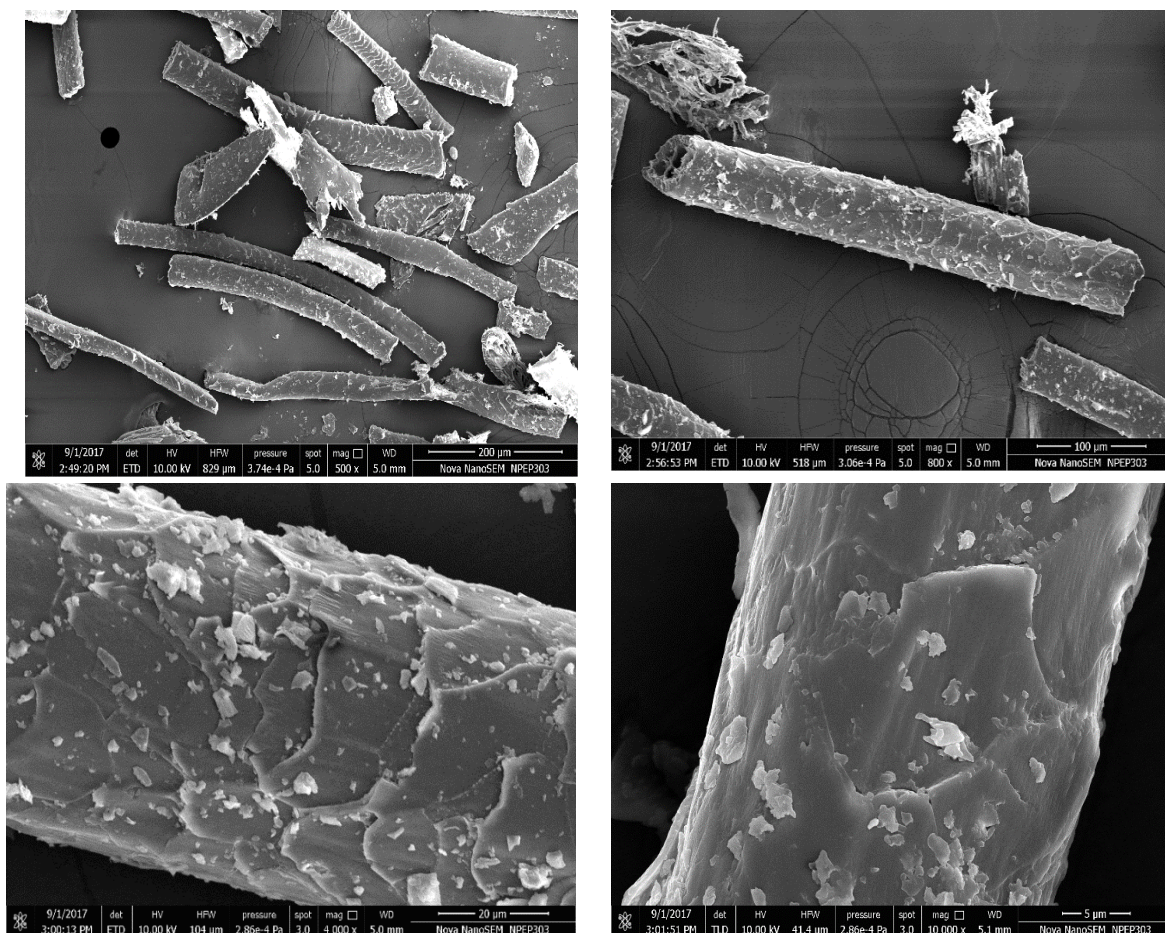

Fig 16: The SEM images of wool particles

The SEM image of the powdered wool-MG composite is shown in **Fig. 17**. The SEM images clearly demonstrate the proper adsorption of MG on powdered wool. This result is attributed to the good homogeneity and fine particle size of the powdered
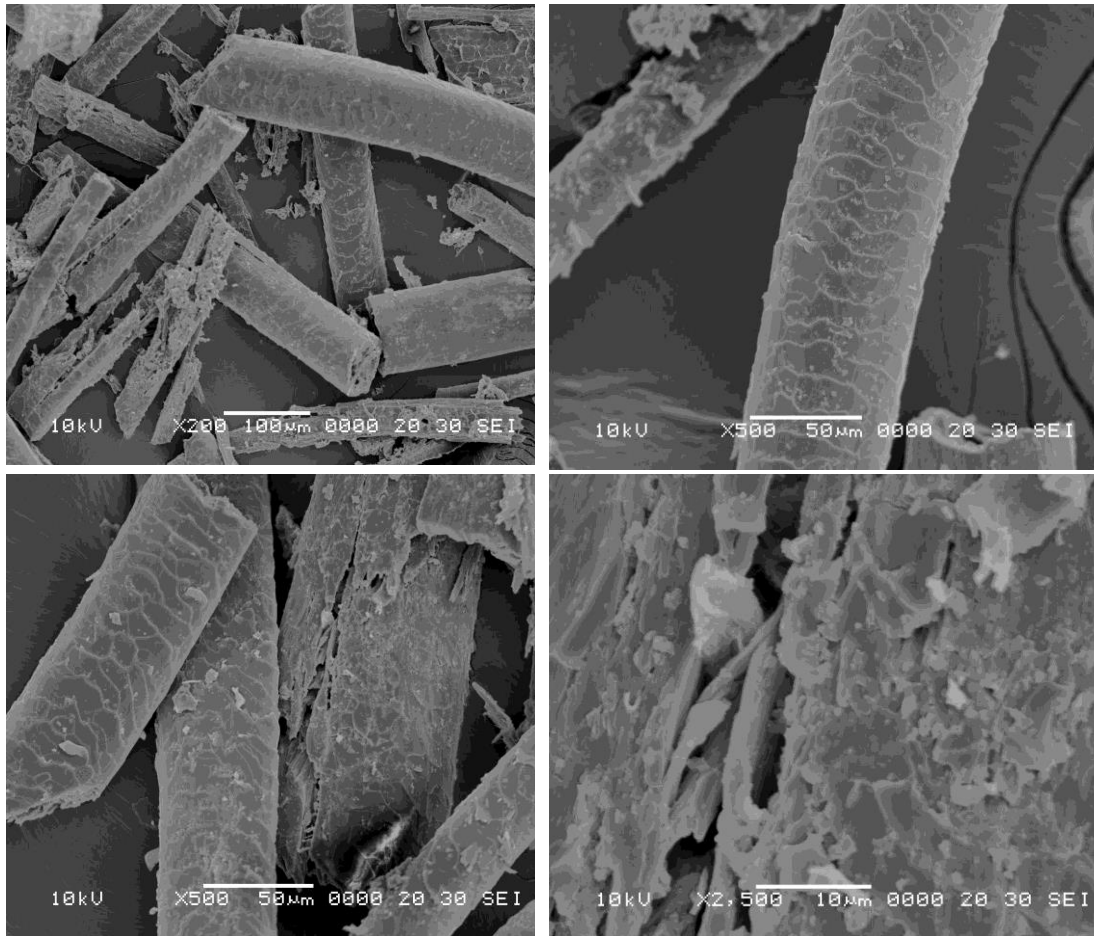
wool.

Fig 17: The SEM images of wool-MG composite

3.2.3. Thermogravimetric analysis (TGA) of fine wool and MG interaction:

To assess heat resistance, thermogravimetric analysis (TGA) was conducted. Figure 18 demonstrates the TGA curve of the fine wool-Malachite Green Oxalate interaction. The analysis was performed under a nitrogen atmosphere, with heating from 30°C to 800°C at a rate of 10°C/min. The mass of the wool-Malachite Green Oxalate composite remained consistent up to 234.89°C, suggesting that the composite maintains thermal stability until this temperature (Fig. 18). At this temperature, weight loss was observed, indicating the beginning of decomposition. The operation required 21.67 minutes. The initial decomposition temperature obtained from TGA was 234.89°C, with a corresponding weight loss of 3.203 mg and a weight loss percentage of 53.74%. The results depict high thermal stability in the case of the wool-Malachite Green Oxalate interaction.
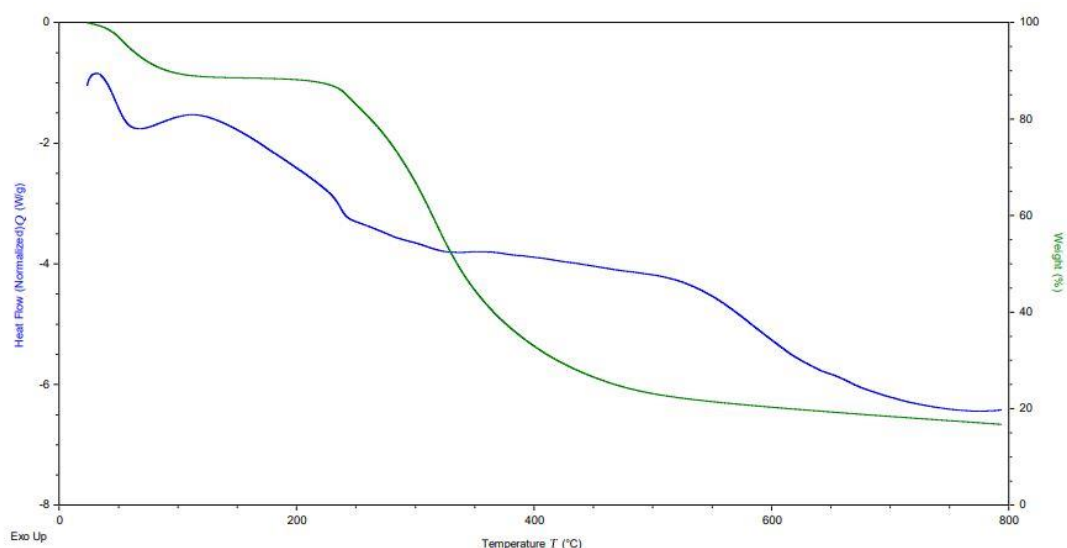
Fig. 18. Thermogravimetric Analysis of Wool-Malachite Green Oxalate composite

3.2.4. Brunauer–Emmett–Teller (BET) *of fine wool:*

The surface area and pore size are very important for fine polymers. The Brunauer–Emmett–Teller (BET) theory is a widely used method to determine the specific surface area and pore size distribution of porous materials. The Brunauer–Emmett–Teller (BET) theory revealed an average pore radius of 1.46029e+02 Å for fine wool, with a surface area of 2.719 m²/g. BET analysis revealed the distribution of pores inside the material and the surface area accessible for adsorption. Fine wool particles, which are porous in nature, offer a large surface area per unit mass due to their complex structure and internal porosity.

4. Conclusion:

Studies clearly revealed the interaction between powdered wool and MG, which effectively eliminates MG from effluent. The interaction proved to be effective at pH 9-10. The data from the Langmuir adsorption equilibrium model fit well. The Freundlich constant (n) was observed to be 5.646 mg L^{-1}, indicating that physisorption is favorable. Pseudo second-order kinetics regulate the adsorption of MG over the wool powder. The negative value of ΔG indicates the spontaneity of the process. The positive value of ΔH indicates the endothermic nature of the process, suggesting chemisorption in the interaction between MG and powdered wool. The MG molecules on solid surfaces exhibited more unpredictability than those in solution, as shown by the positive value of ΔS. Molecular docking confirmed that adsorption is a result of the π-cation interaction between keratin and MG. Nearly 98% of MG dye was adsorbed on fine wool powder at pH 9. The interaction weakened under acidic conditions (pH 2) induced by HCl. Spectrophotometric analysis revealed that about 95% of the dye was recovered from fine wool at pH 2.

5. Conflicts of Interest

No conflict of interest.

6. Author Contributions

KML conducted the investigation, collected data, and wrote the manuscript following statistical analysis. MCN did molecular docking. SNL did data analysis, software analysis. NJK helped conceptualization, methodology. SSS and RKJ helped supervision, reviewing, and editing.

7. References:

1. Ali Khan, M., Govindasamy, R., Ahmad, A., Siddiqui, M. R., Alshareef, S. A., Hakami, A. A. H., & Rafatullah, M. (2021). Carbon based polymeric nanocomposites for dye adsorption: Synthesis, characterization, and application. Polymers, 13(3), 419. https://doi.org/10.3390/polym13030419.
2. Stejskal, J. (2020). Interaction of conducting polymers, polyaniline and polypyrrole, with organic dyes: polymer morphology control, dye adsorption and photocatalytic decomposition. Chemical Papers, 74(1), 1-54. https://doi.org/10.1007/s11696-019-00982-9.
3. Raval, N. P., Shah, P. U., & Shah, N. K. (2017). Malachite green "a cationic dye" and its removal from aqueous solution by adsorption. Applied Water Science, 7, 3407-3445. https://doi.org/10.1007/s13201-016-0512-2.
4. Kushnaryov, V. M., Dunne, W. M., & Buckmire, F. L. (1979). Electron microscopy of Malachite Green—glutaraldehyde fixed bacteria. Stain Technology, 54(6), 331-336. https://doi.org/10.3109/10520297909110693.
5. Rahkonen, R., Koski, P., Shinn, A., Wootten, R., & Sommerville, C. (2002). Post malachite green: Alternative strategies for fungal infections and white spot disease. European Association of Fish Pathologists Bulletin, 22(2), 152-157. http://hdl.handle.net/1893/9955.
6. Brooks, I. J., Walton, S. A., Shmalberg, J., & Harris, A. (2018). Novel treatment using topical malachite green for nasal phaeohyphomycosis caused by a new Cladophialophora species in a cat. Journal of Feline Medicine and Surgery Open Reports, 4(1), 2055116918771767. https://doi.org/10.1177/2055116918771767.
7. Zhang, X., Potty, A. S., Jackson, G. W., Stepanov, V., Tang, A., Liu, Y., ... & Willson, R. C. (2009). Engineered 5S ribosomal RNAs displaying aptamers recognizing vascular endothelial growth factor and malachite green. Journal of Molecular Recognition: An Interdisciplinary Journal, 22(2), 154-161. https://doi.org/10.1002/jmr.917.
8. Oplatowska, M., Donnelly, R. F., Majithiya, R. J., Kennedy, D. G., & Elliott, C. T. (2011). The potential for human exposure, direct and indirect, to the suspected carcinogenic triphenylmethane dye Brilliant Green from green paper towels. Food and Chemical Toxicology, 49(8), 1870-1876. https://doi.org/10.1016/j.fct.2011.05.005.

9. Donya, S. M., Farghaly, A. A., Abo-Zeid, M. A., Aly, H. F., Ali, S. A., Hamed, M. A., & El-Rigal, N. S. (2012). Malachite green induces genotoxic effect and biochemical disturbances in mice. European Review for Medical & Pharmacological Sciences, 16(4).

10. Gharavi-Nakhjavani, M. S., Niazi, A., Hosseini, H., Aminzare, M., Dizaji, R., Tajdar-Oranj, B., & Mirza Alizadeh, A. (2023). Malachite green and leucomalachite green in fish: a global systematic review and meta-analysis. Environmental Science and Pollution Research, 30(17), 48911-48927. https://doi.org/10.1007/s11356-023-26372-z.

11. Srivastava, S., Sinha, R., & Roy, D. (2004). Toxicological effects of malachite green. Aquatic toxicology, 66(3), 319-329. https://doi.org/10.1016/j.aquatox.2003.09.008.

12. Rahman, I. A., Saad, B., Shaidan, S., & Rizal, E. S. (2005). Adsorption characteristics of malachite green on activated carbon derived from rice husks produced by chemical–thermal process. Bioresource technology, 96(14), 1578-1583. https://doi.org/10.1016/j.biortech.2004.12.015.

13. Gupta, V. K., Mittal, A., Krishnan, L., & Gajbe, V. (2004). Adsorption kinetics and column operations for the removal and recovery of malachite green from wastewater using bottom ash. Separation and purification technology, 40(1), 87-96. https://doi.org/10.1016/j.seppur.2004.01.008.

14. Mittal, A. (2006). Adsorption kinetics of removal of a toxic dye, Malachite Green, from wastewater by using hen feathers. Journal of hazardous materials, 133(1-3), 196-202. https://doi.org/10.1016/j.jhazmat.2005.10.017.

15. Nethaji, S., Sivasamy, A., Thennarasu, G., & Saravanan, S. (2010). Adsorption of Malachite Green dye onto activated carbon derived from Borassus aethiopum flower biomass. Journal of hazardous materials, 181(1-3), 271-280. https://doi.org/10.1016/j.jhazmat.2010.05.008.

16. Hameed, B. H., & El-Khaiary, M. I. (2008). Batch removal of malachite green from aqueous solutions by adsorption on oil palm trunk fibre: equilibrium isotherms and kinetic studies. Journal of hazardous materials, 154(1-3), 237-244. https://doi.org/10.1016/j.jhazmat.2007.10.017.

17. Bestani, B., Djourdem, A., Benderdouche, N., & Duclaux, L. (2013). Sawdust-Based Activated Carbon For Malachite Green Removal: Kinetic And Thermodynamic Study. Pro Ligno-Open Access Scientific Journal In The Field **of** Wood Engineering, 9(4), 98-106. https://hal.univ-smb.fr/hal-01814514.

18. Laskar, N., Herbert, A., & Kumar, U. (2023). Application of Taguchi methodology in adsorption of malachite green dye using chemically enhanced Bambusa tulda (Indian timber bamboo). Advances in Environmental Technology, 9(2), 99-111. https://doi.org/ 10.22104/AET.2023.5907.1622.

19. Hameed, B. H., & El-Khaiary, M. I. (2008). Kinetics and equilibrium studies of malachite green adsorption on rice straw-derived char. Journal of Hazardous Materials, 153(1-2), 701-708. https://doi.org/10.1016/j.jhazmat.2007.09.019.

20. Hameed, B. H., & El-Khaiary, M. I. (2008). Malachite green adsorption by rattan sawdust: Isotherm, kinetic and mechanism modeling. Journal of hazardous materials, 159(2-3), 574-579. https://doi.org/10.1016/j.jhazmat.2008.02.054.

21. Hussien Hamad, M. T. M. (2023). Optimization study of the adsorption of malachite green removal by MgO nano-composite, nano-bentonite and fungal immobilization on active carbon using response surface methodology and kinetic study. Environmental Sciences Europe, 35(1), 26.

22. Crini, G., Peindy, H. N., Gimbert, F., & Robert, C. (2007). Removal of CI Basic Green 4 (Malachite Green) from aqueous solutions by adsorption using cyclodextrin-based adsorbent: Kinetic and equilibrium studies. Separation and Purification Technology, 53(1), 97-110. doi:10.1016/j.seppur.2006.06.018.

23. Bekçi, Z., Seki, Y., & Cavas, L. (2009). Removal of malachite green by using an invasive marine alga Caulerpa racemosa var. cylindracea. Journal of hazardous materials, 161(2-3), 1454-1460. DOI: 10.1016/j.jhazmat.2008.04.125.

24. Hamdaoui, O., Saoudi, F., Chiha, M., & Naffrechoux, E. (2008). Sorption of malachite green by a novel sorbent, dead leaves of plane tree: Equilibrium and kinetic modeling. Chemical engineering journal, 143(1-3), 73-84. DOI:10.1016/j.cej.2007.12.018.

25. Shamsizadeh, A., Ghaedi, M., Ansari, A., Azizian, S., & Purkait, M. K. (2014). Tin oxide nanoparticle loaded on activated carbon as new adsorbent for efficient removal of malachite green-oxalate: non-linear kinetics and isotherm study. Journal of Molecular Liquids, 195, 212-218. https://doi.org/10.1016/j.molliq.2014.02.035.

26. Kiani, G., Dostali, M., Rostami, A., & Khataee, A. R. (2011). Adsorption studies on the removal of Malachite Green from aqueous solutions onto halloysite nanotubes. Applied Clay Science, 54(1), 34-39. https://doi.org/10.1016/j.clay.2011.07.008.

27. Kunjiappan, S., Theivendren, P., Pavadai, P., Govindaraj, S., Sankaranarayanan, M., Somasundaram, B., ... & Ammunje, D. N. (2020). Design and in silico modeling of Indoloquinoxaline incorporated keratin nanoparticles for modulation of glucose metabolism in 3T3-L1 adipocytes. Biotechnology Progress, 36(1), e2904. https://doi.org/10.1002/btpr.2904.

28. Manasa, P., & Suhasin, G. (2023). In Silico Molecular Docking Analysis of Selected Natural Biomolecules on Nitric Oxide Synthase. Tropical Journal of Natural Product Research, 7(11). https://doi.org/10.26538/tjnpr/v7i11.34.

29. Hart, A. J., Whalen, P. J., Shin, L. M., McInerney, S. C., Fischer, H., & Rauch, S. L. (2000). Differential response in the human amygdala to racial outgroup vs ingroup face stimuli. Neuroreport, 11(11), 2351-2354.

30. Hamdaoui, O. (2006). Batch study of liquid-phase adsorption of methylene blue using cedar sawdust and crushed brick. *Journal of hazardous materials*, *135*(1-3), 264-273. https://doi.org/10.1016/j.jhazmat.2005.11.062.

31. Bayramoglu, G., Altintas, B., & Arica, M. Y. (2009). Adsorption kinetics and thermodynamic parameters of cationic dyes from aqueous solutions by using a new strong cation-exchange resin. Chemical Engineering Journal, 152(2-3), 339-346. https://doi.org/10.1016/j.cej.2009.04.051.

32. Batzias, F. A., & Sidiras, D. K. (2007). Simulation of dye adsorption by beech sawdust as affected by pH. Journal of Hazardous Materials, 141(3), 668-679. https://doi.org/10.1016/j.jhazmat.2006.07.033.

33. Nanthamathee, C., & Dechatiwongse, P. (2021). Kinetic and thermodynamic studies of neutral dye removal from water using zirconium metal-organic framework analogues. Materials Chemistry and Physics, 258, 123924 https://doi.org/10.1016/j.matchemphys.2020.123924.

34. Li, Q., Chai, L., Yang, Z., Wang, Q., & Wang, Y. (2010). A comparative study of Ag (I) adsorption on raw and modified spent grain: kinetic and thermodynamic aspects. Water environment research, 82(11), 2290-2296. https://doi.org/10.2175/106143010X12681059116978.

35. Khengare, N. J., Labade, S. N., Lalge, K. M., Patil, V. S., Khilare, C. J., & Sawant, S. S. (2022). Effective removal of chromium from aqueous solution by adsorption on powdered wool: In-Silico studies of adsorption mechanism. Chemical Data Collections, 41, 100935. https://doi.org/10.1016/j.cdc.2022.100935.

36. Nagtilak, M., Pawar, S., Labade, S., Khilare, C., & Sawant, S. (2022). Study of the binding interaction between bovine serum albumin and carbofuran insecticide: Multispectroscopic and molecular docking techniques. Journal of Molecular Structure, 1249, 131597. https://doi.org/10.1016/j.molstruc.2021.131597